A Fuzzy-Based Medical Image Fusion Using a Combination of Maximum Selection And Gabor Filters

Fayadh Alenezi, Ezzatollah Salari

Abstract - Medical image fusion (MIF) is important in clinical applications for analysis of diagnostic images. Image fusion (IF) aims to reduce uncertainty and redundancy derived from examining two separate images by creating a single composite image, which is more useful for human interpretation. Fused images have been successfully applied in many other fields including military reconnaissance, target tracking, remote sensing, biometrics, and security systems. Even so, current image fusion techniques have not successfully addressed the poor textual properties and poor edge formation of many resulting fused images. This paper exploits the properties of Gabor filtering and links maximum pixel selection with fuzzy-based image fusion, in order to improve the textual and edge properties of the fused medical images. First, the input images are filtered using Gabor filters, and then pixels with higher intensities are selected before fusion using fuzzy logic. The resultant fused image is superior in textual properties and edge formation compared to those produced by existing methods.

Index terms- Contrast Enhancement, Fuzzy Logic, Gabor Filter, Medical Image Fusion, Maximum Selection

— — — — — — — — ◆ — — — — — — — —

1 INTRODUCTION

Image fusion (IF) has recently been attracting attention from researchers in many different fields. IF is a technique where two or more images with different modalities are combined to form a combined image with more useful information than the originals [1]. Existing methods using IF are being refined and improved as more applications are discovered.

IF techniques typically modify original images on one or more of four different levels, to varying degrees. These four levels are: feature level, signal level, decision level, and pixel level [2]. Most IF methods modify the pixel level, with changes made in either the spatial or transform domain. A set of algorithmic (linear or non-linear) rules are often used in spatial domain methods [3], while the methods using the transform domain require that the images be converted to the transform domain, modified, and then inverted back to the original image domain after fusion [3].

In medical image fusion (MIF), different multi-modal images are fused allowing for visualization of information from different modalities. MIF regularly incorporates pixel-level fusion techniques to create fused images containing useful measurable quantities [5]. Pixel-level fusion is easy to implement and computationally efficient. The most common fusion algorithms utilizing pixel-level techniques include the Average Method, the Maximum Selection Method, the Principle Component Analysis, and the Laplacian Pyramid Method [1, 6].

Multi-modality based diagnostic interpretation is a current standard in medical diagnosis. Use of MIF allows

visualization of different diagnostic, physiologic, and anatomic details, including changes in metabolism, blood flow, regional chemical composition, and absorption [4, 6]. Modalities such as CT, X-ray, DSA, MRI, PET, and SPECT are regularly used in combination to design a diagnostic and a treatment plan for patients. These plans can be enhanced when visualization of fused images is possible.

MIF seeks to combine the most useful information from each modality. For example, Magnetic Resonance Imaging (MRI), Computed Tomography (CT), Ultrasonography (USG), and Magnetic Resonance Angiography (MRA) produce high-resolution images with excellent anatomical detail and precise localization capability [6, 7]. In contrast, Positron Emission Tomography (PET), Single-photon Emission Computed Tomography (SPECT) and functional MRI (FMRI) produce low-spatial-resolution images containing functional information, suitable for the detection of cancer and related metabolic abnormalities, but lacking localization precision.

Image fusion allows information from multiple modalities to be brought together to create a combined, more useful image. For instance, CT images capture the anatomical structure of bone tissues. MRI images show the anatomical structure of soft tissues, organs, and blood vessels. CT and MRI images complement one another and, when combined to form a fused image, offer the most useful information containing details about both hard and soft tissues [5].

Current methods of image fusion, both at the pixel- and transform-domain levels, have inherent limitations. Those using the pixel-level spatial domain yield low-contrast images [9]. Similarly, transform-domain fusion methods based on

multi-scale approaches result in poor edge definition, and are less useful for clinical diagnosis.

Even more recently developed, improved MIF methods suffer from these limitations. For instance, techniques based on intensity-hue-saturation (IHS) and principal component analysis (PCA) demonstrate spectral degradation, compromising their usefulness. Further, IHS deals only with color images and lacks the ability to produce results for black and white source images [7]. Finally, pyramidal image fusion methods, because they lack any spatial orientation selectivity in the decomposition process, result in blocking effects [9, 10].

In fact, each of the existing image fusion approaches has its advantages and disadvantages. For instance, simple averaging fusion techniques, which are the most straightforward and easy to understand algorithms, have unclear fused images [11]. Simple maximum fusion, on the other hand, produces highly focused images, but this results in blurring, which affects the local contrast significantly [12]. Other techniques based on transform-domain fusion techniques such as Discrete Wavelet Transform (DWT), Dual-Tree Complex Wavelet Transform (DT-CWT), and Curvelet Transform, despite their complexity and excellent performance, have shortcomings in handling long curved edges in the image and being more sensitive to the directional information [13]. The widely used Wavelet Transform (WT) technique can preserve spectral information efficiently but cannot express spatial characteristics well, hence salient features of the source images are not preserved efficiently and artifacts and inconsistencies are introduced into the fused results [13, 14, 15].

Recently developed algorithms meant to improve these limitations have met with only limited success. Those based on multi-scale geometric analysis (MGA) tools such as Curvelet, Contourlet, and Ripplet [16, 17] have improved the fused image results in some ways, but they have failed to resolve issues with poor texture and poorly defined edges [18].

Some researchers have noted that the use of fuzzy logic offers solutions to these problems. Fuzzy logic provides the basis for the approximate description of different functions; hence it has found numerous applications in sophisticated systems. Fuzzy transform, which was introduced by [19], can preserve edge formation, remove noise and smooth the images [3]. These properties of fuzzy transform have been applied successfully in image fusion.

This paper proposes a novel method using a fuzzy-based MIF that combines maximum averaging and Gabor filter technology. The proposed method implements a fusion

algorithm whose resultant fused images demonstrated improved edge clarity and texture features, as measured by high standard deviations of pixel values [20, 21]. Our method uses maximum averaging and Gabor filtering, together with fuzzy logic, to create a fused image with very high contrast.

The rest of this paper is organized as follows: section 2 introduces the proposed method, giving a detailed explanation of the tools that will be used. Section 3 shows the simulation results and discusses the results of the simulated outcome. Finally, the conclusion provides a summary of the paper.

2 PROPOSED METHOD
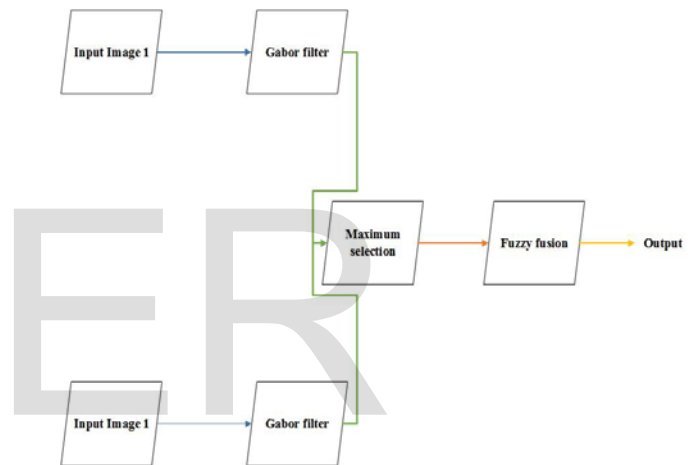
The proposed method is summarized in Figure 1.

Fig 1: The schematic representation of the proposed algorithm.

2.1 Gabor Filter

Gabor filters are seen as sinusoidal planes representable by a Gaussian envelope, making them invariant to illumination, rotation, scale, and translation [22]. Gabor filter is capable of removing noise from the original signals. Gabor filters also possess optimal localization properties in both the spatial and frequency domains. Because of these properties, Gabor filters excel at feature extraction, textual analysis, disparity estimation, and edge detection in image processing and computer vision [23, 24].

Medical images contain dense textural properties, which must be preserved during fusion [25]. We have found Gabor filters in particular to be very useful in implementing our novel MIF. Our technique successfully preserves the textural and edge features so inherently important for diagnostic viewing applications.

The filtering block in Gabor filtering implements one or more convolutions of the images input with 2-D Gabor function represented by the following equations [26, 27, 28, 29]

$$g_{\lambda,\theta,\varphi,\sigma,\gamma}(x,y) = \exp\left(\frac{x'^2 + \gamma^2 y'^2}{2\sigma^2}\right) \cos\left(\frac{2\pi x'}{\lambda} + \varphi\right) \qquad (1)$$

where

$$x' = x\cos\Theta + y\sin\Theta,$$

$$y' = -x\sin\Theta + y\cos\Theta,$$

λ (in our case 3.5) is the wavelength of the sinusoidal factor, Θ is the degrees of orientation of the filter normal to the Gabor function, φ is the phase, σ is the standard deviation of the Gaussian envelope, and γ is the aspect ratio.

Gabor filtering forms the initial stage of the proposed technique. First, a Gabor filter with optimum parameters is created. The optimum parameters chosen in this study are as follows: the filter is set at a 10x10 size with *ktype* values ranging from 0–255 pixels. The orientation angles (θ): 0, 90, 180 and 270 degrees are considered, with γ=1.25, ψ=0, λ=3.5, π=180 and a bandwidth value of 2.8. The images are then converted to gray scale. The texture of the fused image is extracted after transforming the RGB color to YC_bC_r color space, specifically gray color, where the Y value represents the luminance component and the C_bC_r represent the chrominance components of the image. The images are then passed through Gabor filters represented by (1). The maximum results obtained among the four directions are then passed on to the maximum selection stage.

2.2 Maximum Selection

Selecting the appropriate image pixel for the fused image is a critical stage in pixel-level image fusion [30]. Unlike other fuzzy fusion techniques, the selection of a pixel for fusion in our algorithm is based on the centroid of the chosen area, after smoothing or averaging. This procedure ensures that the pixel with maximum intensity is selected and used as the resultant pixel for the fuzzy rules and for the membership sets. In this way, no compromise need be made in separating noise from useful information contained in the original images.

During pixel selection, the pixel intensities for the Gabor filtered images corresponding to the input pairs are compared. A binary selection matrix and its inverse are then generated [26]. The selection matrix is then applied to the first Gabor filtered image, while the inverse selection matrix is applied to the second Gabor filtered image. The resultant pixel values

obtained become the multiple inputs in Fuzzy Interface System (FIS) for the fuzzy logic stage.

2.3 Fuzzy Logic

2.3.1 Fuzzy Logic in Image Fusion

Fuzzy logic exploits human reasoning in natural language to solve uncertainty and redundancy problems [31]. Linguistic terms can be directly encoded as algorithmic rules, which enhance its usability in many applications. For example, it can logically manage unclear boundaries of potential regions of interest. Therefore, fuzzy logic has found applications in areas where uncertainty and no mathematical relationships exist.

In image fusion, fuzzy logic has been used to create more useful images. Fuzzy logic fuses images based on pixel intensities using simple rules that are more easily implemented, compared to other methods [33].

Fuzzy Inference Systems (FIS) are a method of fuzzy logic implementation. FIS models can be either type Mamdani or Sugeno [32]. Mamdani models have constants outputs while Sugeno models permit polynomial outputs. In this paper, only Mamdani fusion models are considered, which corresponds with the pixel-constant output required for image fusion. FIS helps to map from multiple inputs to a single output.

These multiple inputs are converted to linguistic variables before mapping to a single output using a set of predefined membership functions. This process is known as fuzzification and requires the determination of a degree of ownership of each input pixel in reference to a suitable fuzzy set. After fuzzification, the FIS engine is invoked to allow fuzzy operators to be applied to the fuzzified input images to produce the output image. The resulting images for the set of fuzzified input images are then aggregated and defuzzified to produce the final desired output as shown in Figure 2.
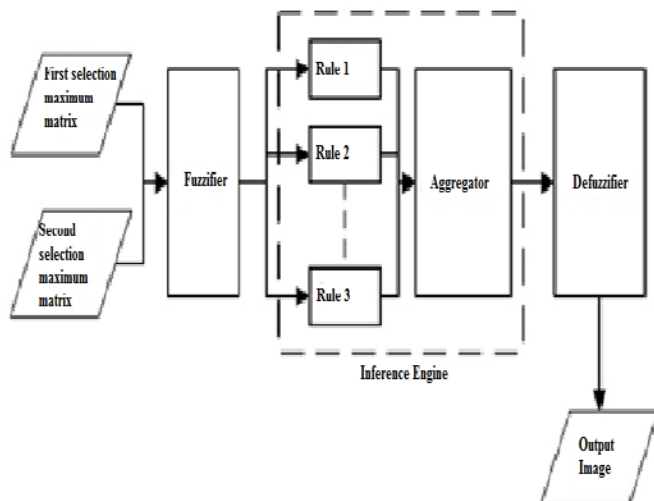
2.3.3   Fuzzy Rules

The fuzzy operator is logical rule based and implemented in the form of IF-THEN statements that determine the pixel value of the result:

$$\text{IF } x \text{ IS } a \text{ AND IF } y \text{ IS } b \text{ THEN } z \text{ IS } c,$$

which can also be represented by

$$I = a \times b \rightarrow c$$

where x is input 1, y is input 2, z is the output and a, b and c are the membership values.

Following the above notations, pixel-wise image fusion also takes a similar course using the following nine rules:

IF (Img 1 IS low) AND (Img 2 IS low) THEN (ImF IS low)

IF (Img 1 IS low) AND (Img 2 IS medium) THE (ImF IS medium)

IF (Img 1 IS low) AND (Img 2 IS high) THEN (ImF IS high)

IF (Img 1 IS medium) AND (Img 2 IS low) then (ImF IS medium)

IF (Img 1 IS medium) AND (Img 2 IS medium) then (ImF is medium)

IF (Img 1 IS medium) AND (Img 2 IS high) THEN (ImF IS high)

IF (Img 1 IS high) AND (Img 2 IS low) THEN (ImF IS high)

IF (Img 1 IS high) AND (Img 2 IS medium) THEN (ImF IS high)

IF (Img 1 IS high) AND (Img 2 IS high) THEN (ImF IS high)

where Img 1 is a pixel for the Gabor filter of image 1 (CT) (or first input), Img 2 is a pixel of the Gabor filter for image 2 (MRI) (or second input), and ImF is the output (fused image).

2.4 Aggregation and Defuzzification

After the fuzzified images are generated, all output is then aggregated according to a maximum selection function:

$$\mu_A(x) = \max\{O_1, O_2, \dots, O_9\}$$

Fig 2: Fuzzy fusion system flow chart

2.3.2   Membership Function

The membership function of a fuzzy set (shown in Figure 3) is defined as a mapping of input pixels from $X \rightarrow [0,1]$. Therefore, fuzzy membership function determines the degree of belonging of each input pixel intensity. Consequently, fuzzy membership function dictates the appropriate fuzzy set for the FIS in the fuzzy logic.

The image pixel values, ranging from 0-255, are segmented into three regions labeled low, medium and high intensity. Resulting regions can be characterized as linguistic variables for use as fuzzy set membership functions. They are defined as:

$$U = \{low, medium, high\}$$

where low, medium and high are used as the regions, with each representing membership functions.
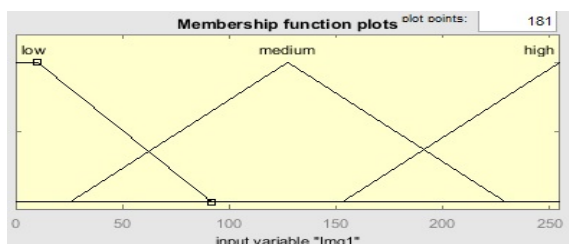

Fig 3: Membership functions

The maximum function is used to unify the outputs where $\mu_A(x)$ is the aggregated curve and O_k for $k = 1,2,3,...,9$ is the output for the k-th rule. The output is then defuzzified using the centroid of area (COA), to give the desired pixel values for the fused image. COA is given by:

$$X_{COA} = \frac{\int \mu_A(x)xdx}{\int \mu_A(x)dx} \qquad (2)$$

3 SIMULATION RESULTS

3.1 Experimental Setup

The proposed technique, which was implemented in MATLAB R2016b, was evaluated using three different sets of images as examples, presented in Figures 4, 5, and 6. The experiments were conducted using Gabor filtering in four directions: $\theta = 0^0, 90^0, 180^0,$ and 270^0; the results are presented in Figures 4, 5, and 6 along with performance measurements as shown in tables 1, 2, and 3. The best result from each example was compared with images created by other researchers using existing fusion techniques, presented in Table 4 and Figure 7. The criteria used in the performance evaluation of various algorithms as presented in table 4 are the standard deviation, root mean square error (RMSE) and entropy measures. The standard deviation is a measure of the contrast and textual properties and edge formation of the image [34]. Images with high standard deviation have better improved textual properties and better edge formation. The RMSE is a measure of the amount of change per pixel due to

the processing. The lower the RMSE, the lower the level of noise in the image, meaning the better the image formation. The entropy is a measure of image quality in terms of information content. The higher the entropy, the better the image quality, i.e., the more information the image contains.

The criterion used in the selection of the best output presented in Table 4 is based on the output with either the lowest value of RMSE, or the highest value of standard deviation or entropy. However, it must be noted that entropy values played an insignificant role in the selection of the outputs presented in Table 4. This is because the proposed technique focuses on improving textual properties and proper edge formation. Images with improved textual properties and edge formation are characterized by higher standard deviation values and lower RMSE.

Figure 4 shows the input images in the first column (CT and MRI images), Gabor filtered images under different orientations (θ is 0, 90, 180 and 270 degrees) are shown in the second to fifth columns, and the corresponding fused images are in the last rows for example 1.
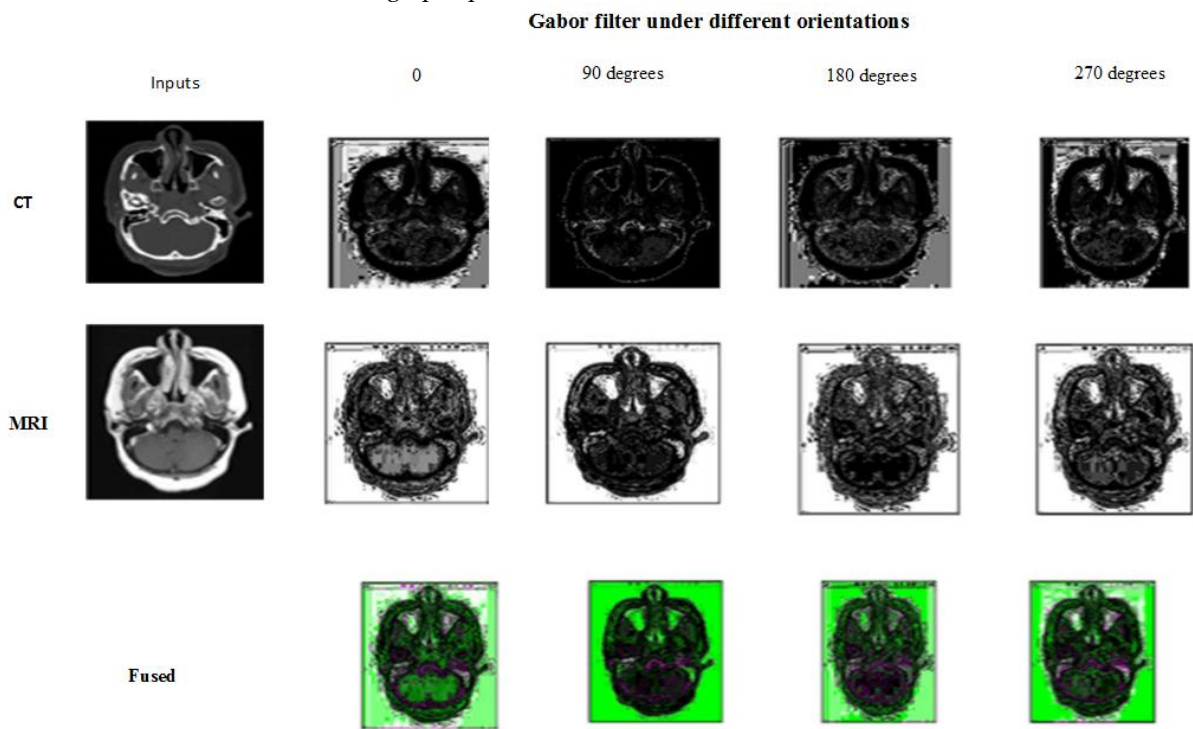

Gabor filter under different orientations

Fig 4: Inputs and Gabor filtered outputs under different orientations, and resultants fused images for example 1.

Table 1: Performance evaluation measures for example 1 under different orientations of Gabor filter.

Performance evaluation measures	Values at different directions (θ)			
	0°	90°	180°	270°
Entropy	4.3803	3.4507	4.0254	4.0502
Standard deviation	102.9260	117.7324	109.3426	111.9463
RMSE	0.1003	0.0736	0.1098	0.0960

Figure 5 shows the input images in the first column (CT and MRI images), Gabor filtered images under different orientations (θ is 0, 90, 180 and 270 degrees) in the second to fifth columns, and the corresponding fused images in the last rows for example 2.
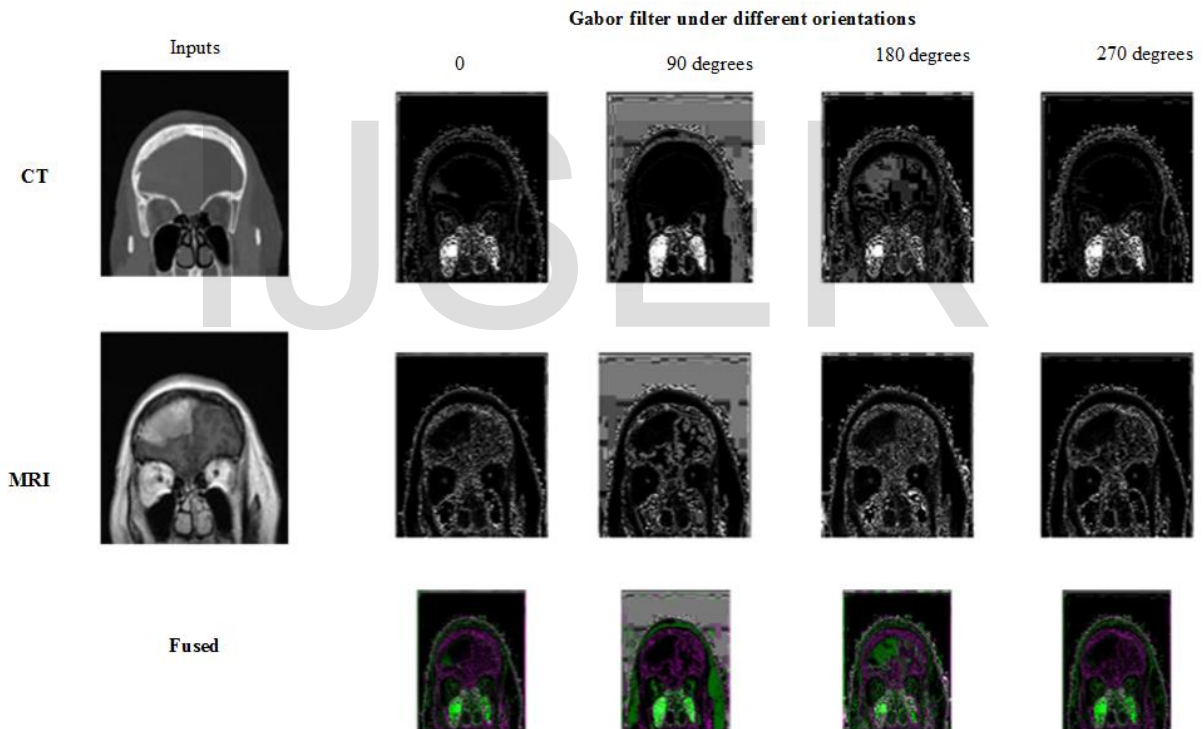

Fig 5: Input images and Gabor filtered outputs under different orientations, and resultants fused images for example 2.

Table 2: Performance evaluation measures for example 2 under different orientations of Gabor filter

Performance-evaluation measures	Values at different directions (θ)			
	0°	90°	180°	270°

Entropy	3.4935	4.2900	3.8054	3.4524
Standard deviation	120.4455	106.1650	118.0412	120.7756
RMSE	0.0942	0.0852	0.1026	0.0886

Figure 6 shows the input images in the first column (CT and MRI images), Gabor filtered images under different orientations (θ is 0, 90, 180 and 270 degrees) in the second to fifth columns, and the corresponding fused images in the last rows for example 3.
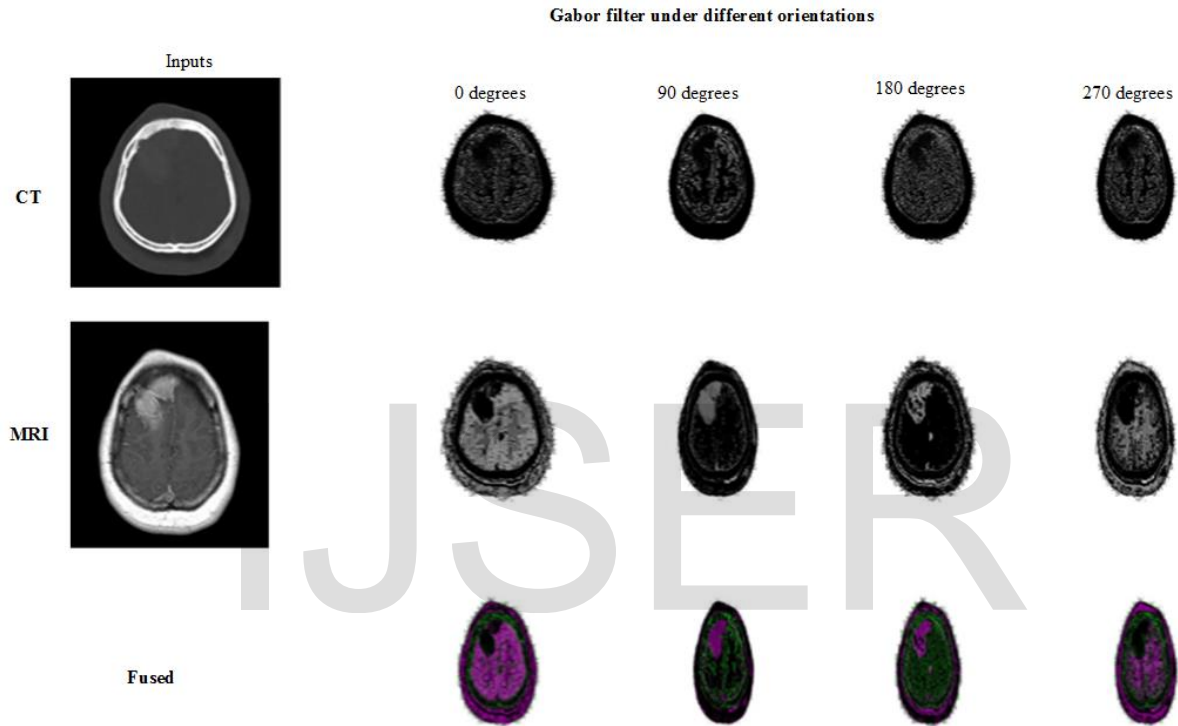

Fig 6: Input images and Gabor filtered outputs under different orientations, and resultants fused images for example 3.

Table 3: Performance evaluation measures for example 3 under different orientations of Gabor filter.

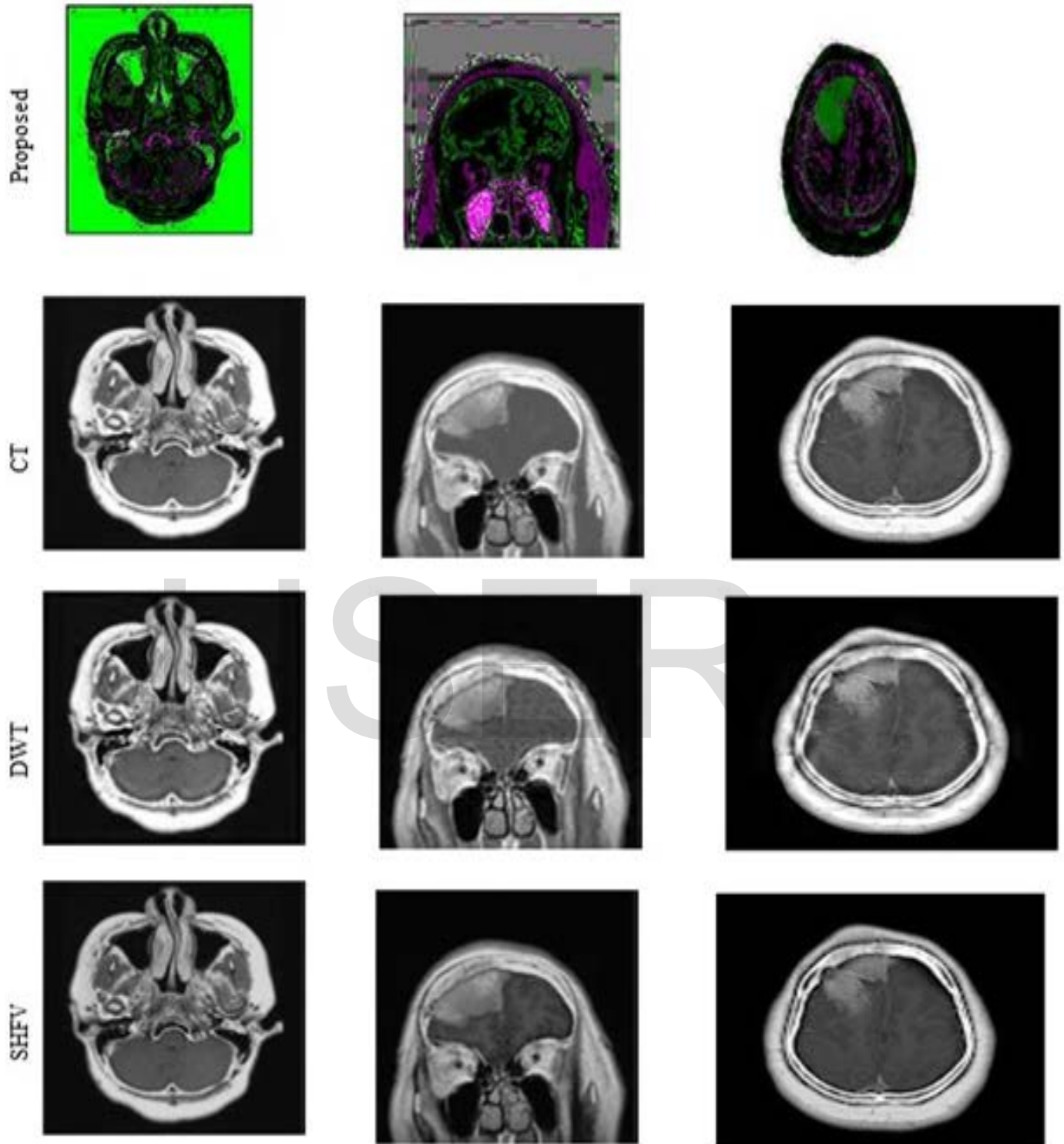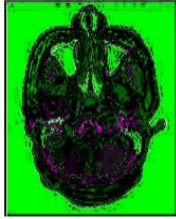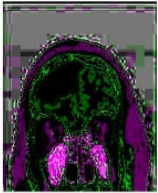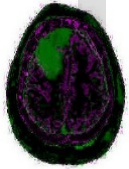| Performance evaluation measures	Values at different directions (θ)			
	0°	90°	180°	270°
Entropy	2.7584	2.4584	2.3886	2.6969
Standard deviation	85.0618	94.5942	94.6862	89.202
RMSE	0.0706	0.0446	0.0774	0.0643

Fig 7: Comparison of results with other image fusion techniques.

Table 4: Tabulated results in comparison with the existing techniques.

Examples	Algorithm	Entropy	Standard Deviation	RMSE	Source
	Proposed	3.4507	117.7324	0.0736	
	Contourlet Transform (CT)	7.1332	54.1504	0.1662	[35]
	Discrete wavelet (DWT)-Method	6.9543	47.2304	0.2703	[35]
	Shearlets and Human Feature	7.6572	56.7993	0.1164	[35]
	Proposed	3.8054	118.0412	0.1026	
	CT	6.9351	46.6294	0.2538	[35]
	DWT	6.6997	41.4623	0.2889	[35]
	SHFV	7.3791	55.8533	0.2410	[35]
	Proposed	2.3886	94.6862	0.0774	
	CT	6.8824	43.1963	0.2422	[35]
	DWT	6.5198	42.0087	0.3142	[35]
	SHFV	6.9467	44.2937	0.2133	[35]

3.2 Discussion

Our experimental results have proven to be highly applicable in the field of diagnostic medicine, where improved textual surface appearance is critical.

The fused images obtained from the other existing techniques as presented in Table 4 and Figure 7 suggest that our method is objectively superior. The proposed technique focuses on fused results with high textual properties and improved edge information in the resulting fused image. These improvements are demonstrated in the measurement of high values of standard deviation and lower values of RMSE.

of standard deviation obtained by the proposed technique show that it performs better than others. The lowest RMSE values prove that the technique produces images with lower noise, and hence improves image quality. In terms of entropy,

Examples presented in Table 4 shows that the fused images created using our technique have the highest standard deviation values, indicating better textual properties and improved edge information. Higher standard deviations are also associated with higher contrast. As the numbers suggest, the proposed fusion method yields images with a better contrast assisting physicians for medical diagnostic applications.

Evaluated in terms of the desired objectives, the proposed method gives better results, meaning it outperforms the existing methods as evidenced in Table 4. The highest values

the existing methods had higher values. However, it must be recalled that the objective of the proposed method was to produce images with higher textual properties and better edge information, which is evident in low RMSE and high standard

deviation values. Thus, in terms of the objective evaluation criterion, the proposed method is better than the comparison techniques.

The better results obtained from the proposed method indicate the influence of Gabor filtering on the input images before fusion. This makes sense, because it is known that Gabor filters remove noise in images, resulting in images with superior textual properties and edges with longer curves. Edges with longer curves indicate better edge information, which still shows better textual properties. Images with longer curves on the edges and higher textual properties are easier to analyze during clinical diagnosis.

4. CONCLUSION

This paper has presented a novel medical image fusion method based on fuzzy logic with a combination of maximum averaging selection with Gabor filtering. Prior medical image fusion techniques have produced images with high entropy, while the standard deviation is low and RMSE is high. This means they have low perceptual quality, in terms of the textual properties and edge information, both of which are important in the visualization of patterns in the images. The proposed technique was able to improve the textual properties and edge information of fused images by exploiting the properties of Gabor filtering, fuzzy logic, and maximum selection to create more useful images for diagnosis. The study linked the Gabor filter properties and maximum selection algorithm with a fuzzy logic approach to produce fused images, which are more appropriate in assisting physicians to make accurate medical diagnoses. The resulting images, which combine low information content with better textual properties and edge information, should propel future studies of the proposed technique.

REFERENCES

[1] J. M. C. Rodriguez, S. Mitra, S. M. Thampi and E.-S. El-Alfy, Intelligent Systems Technologies and Applications 2016, vol. 530, Springer, 2016.

[2] B. Kisacanin, S. S. Bhattacharyya and S. Chai, Embedded computer vision, Springer Science \& Business Media, 2008.

[3] T. Huang, Z. Zeng, C. Li and C. S. Leung, Neural Information Processing: 19th International Conference, ICONIP 2012, Doha, Qatar, November 12-15, 2012, Proceedings, Springer, 2009.

[4] C. Yi and Y. Tian, "Text detection in natural scene images by stroke gabor words," in *Document Analysis and Recognition (ICDAR), 2011 International Conference on*, 2011.

[5] V. P. S. Naidu and J. R. Raol, "Pixel-level image fusion using wavelets and principal component analysis," *Defence Science Journal,* vol. 58, no. 3, p. 338, 2008.

[6] N. A. Al-Azzawi, "Medical Image Fusion based on Shearlets and Human Feature Visibility," *International Journal of Computer Applications,* vol. 125, no. 12, pp. 1-12, 2015.

[7] N. Petkov and M. Wieling, "Gabor filter for image processing and computer vision," University of Groningen, Department of Computing Science, Intelligent Systems, 2008.

[8] G. T. Shrivakshan and C. Chandrasekar, "A comparison of various edge detection techniques used in image processing," *IJCSI International Journal of Computer Science Issues,* vol. 9, no. 5, pp. 272-276, 2012.

[9] A. H. Kulkarni and R. A. Patil, "Applying image processing technique to detect plant diseases," *International Journal of Modern Engineering Research (IJMER),* vol. 2, no. 5, pp. 3661-3664., 2012.

[10] S. Das and M. K. Kundu, "A neuro-fuzzy approach for medical image fusion," *IEEE transactions on biomedical engineering,* vol. 60, no. 12, pp. 3347-3353, 2013.

[11] V. S. Petrovic and C. S. Xydeas, "Gradient-based multiresolution image fusion," *IEEE Transactions on Image processing,* vol. 13, no. 2, pp. 228-237, 2004.

[12] H. B. Mitchell, Image fusion: theories, techniques and applications, Springer Science & Business Media, 2010.

[13] S. Kuruvilla and J. Anitha, "Comparison of registered multimodal medical image fusion techniques," in *Electronics and Communication Systems (ICECS), 2014 International Conference on*, 2014.

[14] P. S. Swathi, M. S. Sheethal and V. Paul, "Survey on Multimodal Medical Image Fusion Techniques," *International Journal of Science, Engineering and Computer Technology,* vol. 6, no. 1, p. 33, 2016.

[15] H. M. a. R. E.-S. M. E. El-Hoseny, W. A. Elrahman and F. E. A. El-Samie, "Medical image fusion techniques based on combined discrete transform domains," in *Radio Science Conference (NRSC), 2017 34th National*, 2017.

[16] R. Kaur and S. Kaur, "An Approach for Image Fusion using PCA and Genetic Algorithm," *Image,* vol. 15, no. 16, 2016.

[17] V. P. Tank, D. D. Shah, T. V. Vyas, S. B. Chotaliya and M. S. Manavadaria, "Image Fusion Based On Wavelet And Curvelet Transform," *IOSR Journal of VLSI and Signal Processing (IOSR-JVSP) ISSN,* vol. 1, no. 5, pp. 32-36, Jan-Feb 2013.

[18] P. Ashishgoud and G. Usha, "Image Fusion Using DWT & PCA," *International Journal of Advanced Research in Computer Science and Software Engineering,* vol. 5, no. 4, pp. 800-804, 2015.

[19] R. C. Gonzalez, R. E. Woods and others, *Digital image processing,* Addison-wesley Reading, 1992.

[20] J.-K. Kamarainen, V. Kyrki and H. Kalviainen, "Invariance properties of Gabor filter-based features-overview and applications," *IEEE Transactions on image processing,* vol. 15, no. 5, pp. 1088-1099, 2006.

[21] S. R. Dammavalam, S. Maddala and M. H. M. Prasad, "Quality Assessment of Pixel-Level ImageFusion Using Fuzzy Logic," *International Journal on Soft Computing,* vol. 3, no. 1, pp. 11-23, February 2012.

[22] R. Maruthi and K. and Sankarasubramanian, "Pixel level multifocus image fusion based on fuzzy logic approach," *Asian Journal of Information Technology,* vol. 7, no. 4, pp. 168-171, 2008.

[23] L. Singh, S. Agrawal and P. Gupta, "Review on medical image fusion based on neuro-fuzzy," *International Journal of Scientific Research Engineering & Technology (IJSRET),* vol. 4, no. 7, pp. 777-781, July 2015.

[24] S. Rajkumar, P. Bardhan, S. K. Akkireddy and C. Munshi, "CT and MRI image fusion based on Wavelet Transform and Neuro-Fuzzy concepts with quantitative analysis," in *Electronics and Communication Systems (ICECS), 2014 International Conference on,* 2014.

[25] H. Yang, Y. Fang and W. Lin, "Perceptual quality assessment of screen content images," *IEEE Transactions on Image Processing,* vol. 24, no. 11, pp. 4408-4421, 2015.

[26] L. Li, Y. Yan, Y. Fang, S. Wang, L. Tang and J. Qian, "Perceptual quality evaluation for image defocus deblurring," *Signal Processing: Image Communication,* vol. 48, pp. 81-91, 2016.

[27] D. Kesavan, E. Philip, L. Emmanuel, P. K. Philip and S. R. Mathew, "Fuzzy Logic based Multi-modal Medical Image Fusion of MRI-PET Images," *International Journal of Science Technology & Engineering,* vol. 2, no. 10, pp. 268-271, 2016.

[28] M. Manchanda and R. Sharma, "A novel method of multimodal medical image fusion using fuzzy transform," *Journal of Visual Communication and Image Representation,* vol. 40, pp. 197-217, 2016.

[29] J. M. Patel and M. C. Parikh, "Medical image fusion based on Multi-Scaling (DRT) and Multi-Resolution (DWT) technique," in *Communication and Signal Processing (ICCSP), 2016 International Conference on,* 2016.

[30] I. Perfilieva, "Fuzzy transforms: Theory and applications," *Fuzzy sets and systems,* vol. 157, no. 8, pp. 993-1023, 2006.

[31] C. H. Seng, A. Bouzerdoum, F. H. C. Tivive and M. G. Amin, "Fuzzy logic-based image fusion for multi-view through-the-wall radar," in *Digital Image Computing: Techniques and Applications (DICTA), 2010 International Conference on,* 2010.

[32] M. Mas, M. Monserrat, J. Torrens and E. Trillas, "A survey on fuzzy implication functions," *IEEE Transactions on fuzzy systems,* vol. 15, no. 6, pp. 1107-1121, 2007.

[33] H. Singh, J. Raj, G. Kaur and T. Meitzler, "Image fusion using fuzzy logic and applications," in *Fuzzy Systems, 2004. Proceedings. 2004 IEEE International Conference on,* Budapest, Hungary, 2004.

[34] I. De and B. Chanda, "A simple and efficient algorithm for multifocus image fusion using morphological wavelets," *Signal Processing,* vol. 86, no. 5, pp. 924-936, 2006.

[35] G. Selvakumari and R. Aravindh, "A New Medical Image Fusion based on Non-Subsampled Contourlet Transform," *Journal of Computer Applications (JCA),* vol. 7, no. 1, p. 2014, 2014.